Journal of Molecular Catalysis B: Enzymatic xxx (2017) xxx–xxx

Contents lists available at ScienceDirect

Journal of Molecular Catalysis B: Enzymatic

journal homepage: www.elsevier.com/locate/molcatb

# Biocatalytic study of novel oleate hydratases

Jens Schmid [1], Lisa Steiner [1], Silvia Fademrecht, Jürgen Pleiss, Konrad B. Otte, Bernhard Hauer*

*Institute of Technical Biochemistry, University of Stuttgart, Allmandring 31, D-70569 Stuttgart, Germany*

ARTICLE INFO

*Article history:*
Received 18 October 2016
Received in revised form 10 January 2017
Accepted 11 January 2017
Available online xxx

*Keywords:*
Alkenes
Biocatalysis
Database analysis
Hydration
Oleate hydratases

ABSTRACT

The direct hydration of C=C bonds to yield alcohols or the reverse dehydration is chemically challenging but highly sought after. Recently, oleate hydratases (OAHs) gained attention as biocatalytic alternatives capable of hydrating isolated, non-activated C=C bonds. Their natural reaction is the conversion of oleic acid to (*R*)-10-hydroxystearic acid.

In this work, we report the first comparative study of several OAHs. Therefore we established the *Hydratase Engineering Database* (HyED) comprising 2046 putative OAHs from eleven homologous families and selected nine homologs for cloning in *E. coli*. The heterologously expressed enzymes were evaluated concerning activity and substrate specificity. The enzymes have a broad substrate scope ranging from oleic acid (C18) to the novel synthetic substrate (*Z*)-undec-9-enoic acid (C11). The OAHs from *Elizabethkingia meningoseptica* and *Chryseobacterium gleum* showed the best expression, highest stability and broadest substrate scope, making them interesting candidates for directed evolution to engineer them for the application as general hydratase catalysts.



## 1. Introduction

In recent years, hydratases received increasing attention as possible biocatalysts, as they enable the regio- and stereoselective addition of water to double bonds or the reverse water elimination. Chemical hydrations require harsh acidic conditions, which lead in general to a broad range of side-reactions and a significant loss of selectivity [1].

Hydratases are classified as hydro-lyases (EC 4.2.1) and can be divided into two groups regarding their substrates and need of cofactors [2,3]. Cofactor-dependent hydratases add water to activated α,β-unsaturated carbonyl compounds, whereas hydratases acting on isolated carbon–carbon double bonds are described to be cofactor-independent [3,4]. Rare examples for the latter group are the carotenoid hydratase [5,6], the linalool dehydratase-isomerase [7] and the oleate hydratase (OAH) [8].

OAHs (EC 4.2.1.53) are promising biocatalysts for the selective addition of water to C=C bonds. They were first described by Wallen *et al.* in 1962 when they found *Elizabethkingia meningoseptica* (formerly known as *Pseudomonas* sp. strain 3266) capable of hydrating oleic acid to 10-hydroxystearic acid [9]. Since then, a number of other strains were found to possess OAHs and several studies have been performed on the selectivity, the kinetics and the mechanism of the reaction [8]. Isotope labeling experiments confirmed that the alcohol group was introduced at the C-10 position [10]. Schroepfer and Bloch showed that the hydroxyl group is formed stereoselectively in (*R*)-configuration [11]. They also proved that the reaction does not take place via an initial epoxidation and subsequent reductive opening by conducting the reaction under anaerobic conditions. Furthermore, the utilization of 9,10-epoxyoctadecanoic acid as precursor did not lead to the formation of 10-hydroxystearic acid [12,13]. Other studies on novel fatty acid hydratases also addressed regioselectivity. For instance, the hydratase from *Micrococcus caseolyticus* was most active for oleic acid indicating that it was an OAH, however, hydration also occurred at *cis*-12 C=C bonds [14]. Only in 2015, a second hydratase from *Lactobacillus acidophilus* (*La*) was discovered, catalyzing the addition of water selectively to the 12*Z*-position [15]. In previous studies, however, it was reported that most hydratases add water exclusively to the 9*Z*-double bond, with the hydroxyl group being introduced at the C-10 atom [8,16–18].

*Abbreviations:* C=C, carbon–carbon double bond; OAH(s), oleate hydratase(s); HyED, *Hydratase Engineering Database*; HFam(s), homologous family/families; gDNA, genomic DNA; *Cg*, *Chryseobacterium gleum*; *Db*, *Desulfomicrobium baculatum*; *Em*, *Elizabethkingia meningoseptica*; *Gm*, *Gemella morbillorum*; *Ht*, *Haloterrigena thermotolerans*; *La*, *Lactobacillus acidophilus*; *Lj*, *Lactobacillus johnsonii*; *Mp*, *Mucilaginibacter paludis*; *Tt*, *Thermoanaerobacterium thermosaccharolyticum*.

* Corresponding author.
*E-mail address:* Bernhard.Hauer@itb.uni-stuttgart.de (B. Hauer).

[1] These authors contributed equally to this work

http://dx.doi.org/10.1016/j.molcatb.2017.01.010
1381-1177/

The first OAH was isolated in 2009 from *Elizabethkingia meningoseptica* (*Em*-OAH1), subsequently cloned in *E. coli* and biochemically characterized [8]. Recently, the crystal structures of *La*-OAH1 and *Em*-OAH1 were solved, giving more insight into the FAD binding and the reaction mechanism [18,19]. It was revealed that the *Em*-OAH1 is a dimer and each monomer contains not only a $Ca^{2+}$-ion but also FAD as prosthetic group. However, the exact function of FAD still remains unclear. A structural or mechanistic purpose has been discussed [18,19].

Since the first OAH was described, several hydratases from different organisms followed, but were in most cases not characterized in detail. Nevertheless, OAHs are successfully applied in larger-scale biotransformations of unsaturated fatty acids (mainly oleic acid) [1]. The resulting hydroxy fatty acids and their derivatives are applied in a broad range from detergents and paintings to biopolymers and flavor compounds [2,20,21]. Beside the production of 10-hydroxystearic acid, OAHs have also been embedded in cascade reactions for the synthesis of plastic monomers (α,ω-dicarboxylic acids for polyesters and amino acids for polyamides) from renewable fatty acids [1,22,23]. Moreover, the enzymatic dehydration of short chain alcohols (e. g. isobutanol) was described [2,24].

As most of the described enzymes were investigated with divergent substrate panels (ranging from saturated to polyunsaturated fatty acids with a chain length from C12 to C22) and with different reaction set-ups (*in vitro* or *in vivo*), it is difficult to directly compare the different enzymes [4].

Herein, we present the compilation of a comprehensive database and activity assessment of nine representative hydratases from three different homologous families with varying similarities on one profound substrate panel. In combination with the investigation of the enzymes' stability and their capability to be overexpressed in *E. coli*, this study aims for the identification of an ideal starting candidate for directed mutagenesis as well as the generation of new insights into the growing OAH family.

## 2. Experimental

### 2.1. Chemicals & DNA

The chemicals were purchased from the following suppliers: Sigma-Aldrich (St. Louis, USA), Serva (Heidelberg, DE), Merck (Darmstadt, DE), Peqlab (Erlangen, DE), Alfa Aesar (Karlsruhe, DE), Carl Roth (Karlsruhe, DE) and Macherey-Nagel (Düren, DE).

Genomic DNA (gDNA) as a source of desired OAH genes was obtained from DSMZ (Leibniz-Institut, Braunschweig, DE). Oligonucleotides were obtained from Metabion (Planegg, DE).

### 2.2. Database setup

The *Hydratase Engineering Database* (HyED) was established within our in-house database system BioCatNet [25] based on 20 sequences (Table S1) derived from a hydratase patent by Marliere describing the dehydration of alcohols for the production of alkenes [24]. A BLAST search in the non-redundant protein database of the NCBI was performed for each of these sequences using an expectation threshold of $10^{-10}$ [26,27]. Hits sharing a sequence identity of >98 % were assigned to a single protein entry. Homologous families were automatically generated by clustering all sequences with USEARCH and an identity cut-off of 50 % [28]. For further classifications into superfamilies, all sequences were compared using the Needleman-Wunsch algorithm [29] for pairwise sequence alignments. Similarities were visualized using sequence similarity networks generated with Cytoscape version 3.2.1 and the organic layout (Fig. 1) [30]. Available structures were downloaded from the Protein Data Bank (PDB) and stored in the respective protein entry [31]. The *Hydratase Engineering Database* is publicly available at https://hyed.biocatnet.de and can be browsed by sequence, structure or source organism. All sequences, multiple sequence alignments and phylogenetic trees can be accessed online or be downloaded.

### 2.3. Conservation analysis

For identification of conserved positions, a multiple sequence alignment of all sequences of the database was calculated using Clustal Omega [32]. For each alignment column, the occurrence of each amino acid was counted. Positions were considered to be conserved if one or two amino acids were found in >90 % of all sequences.

### 2.4. Cloning of homologous enzymes

The OAH genes were amplified from gDNA via PCR (see Table S2 for primers, Tables S3, S5 and S7 for reaction mixture and Tables S4, S6 and S8 for temperature program). pET28a(+) was used as vector backbone. For the cloning of *La*- and *Lj*-OAH1, the *Nco*I restriction site in pET28a(+) was changed to *Nde*I by using the ligation-during-amplification method. *Cg*-OAH1 was ligated into pET28a(+) using the *Xba*I and *Xho*I restriction sites. For *Db*-, *Em*-, *Gm*-, *Mp*- and *Tt*-OAH1 *Nco*I and *Xho*I were used. For *Ht*-OAH1 *Xba*I and *Hin*dIII, for *La*- and *Lj*-OAH1 the restriction sites *Nde*I and *Xho*I were used.

### 2.5. Expression of hydratase genes

A preculture of *E. coli* BL21 (DE3) containing the corresponding plasmid was used to inoculate a 2 L baffled flask containing 400 mL TB medium and kanamycin (final concentration: 30 μg $mL^{-1}$) to an $OD_{600}$ of 0.05. The cultures were incubated at 37 °C and 180 rpm until an $OD_{600}$ of 0.5 was reached. Expression was induced by adding 0.5 mM IPTG at 20 °C. After 16 h at 20 °C and 140 rpm the cells were harvested by centrifugation (30 min, 20,450 × *g*, 4 °C) and the pellet was stored at −20 °C until further use.

Cell disruption was achieved either by sonication or chemical lysis. For sonication, a cell suspension (10 mL $g^{-1}$ cell pellet in the same buffer as used for reaction) was prepared and kept on ice during disruption using a Branson Sonifier 250 (5 cycles: 1 min on/45 s off, duty cycle 30 %, output 4). Lysate was obtained by centrifugation (20 min, 894 × *g*, 4 °C) as supernatant. For chemical lysis, harvested cells were resuspended at room temperature in 5 mL $g^{-1}$ 1 x BugBuster Protein Extraction Reagent (Merck, Darmstadt, DE) to which a spatula tip of DNase was added. The suspension was shaken (20 min, 25 °C, 300 rpm) and subsequently centrifuged (20 min, 16,000 × *g*, 4 °C).The protein concentration was determined by bicinchoninic acid assay kit (Pierce BCA Protein Assay Kit, Thermo Scientific, Waltham, USA) according to manufacturer's microwell plate protocol and the lysate was analyzed by SDS-PAGE (according to Laemmli [33]).

Therefore, the obtained lysate was diluted to a concentration of 2 g $L^{-1}$ and mixed with the same volume of 2 x SDS sample buffer (2 mL 1 M TRIS/HCl pH 6.8; 190 mg $MgCl_2$; 1 mL glycerol; 0.8 g SDS; 2 mg bromophenol blue; 310 mg DTT, water ad to 20 mL). Whole cell samples were taken during or after expression normalized to $OD_{600}$ = 0.25 and resuspended in 50 μL 2 x SDS sample buffer. Both, whole cell and lysate samples, were denatured at 95 °C for 10 min. Denatured samples were loaded (10 μL for lysate, 15 μL for pellets) on the gels along with 5 μL PageRuler Prestained Protein Ladder (Thermo Scientific, product # 26616).

Please cite this article in press as: J. Schmid, et al., Biocatalytic study of novel oleate hydratases, J. Mol. Catal. B: Enzym. (2017), http://dx.doi.org/10.1016/j.molcatb.2017.01.010

### 2.6. Biotransformations and analytics

For characterization of the enzymes, biotransformations were performed in triplicates and conducted on 500 μL-scale in 1.5 mL reaction tubes. Protein concentrations and reaction times are listed in Table 1. Negative controls were performed using lysate of cells containing empty pET28a(+) vector. All reactions were performed in 50 mM potassium phosphate buffer pH 6.5 except for biotransformations of (*Z*)-undec-9-enoic acid and dec-9-enoic acid, which were performed in 50 mM citrate buffer pH 6. Substrate was added to a final concentration of 500 μM. The reaction mixture was shaken at 25 °C and 600 rpm. The reaction was quenched by the addition of 20 μL 1 M HCl, extracted two times with 500 μL methyl *tert*-butyl ether (MTBE) and 100 μM internal standard (heptadecanoic acid for linoleic acid, oleic acid and palmitoleic acid or pentadecanoic acid for myristoleic acid, (*Z*)-undec-9-enoic acid and dec-9-enoic acid). The organic phase was concentrated *in vacuo* and the residue derivatized using 40 μL *N,O*-bis(trimethylsilyl)trifluoroacetamide containing 1 % trimethylchlorosilane.

Derivatized samples were analyzed on a Shimadzu GC2010 Plus (Shimadzu, Kyōto, JP) equipped with an AOC 20 s autosampler, AOC 20i autoinjector (injection volume: 1 μL, split ratio: 1:10, injection temperature: 250 °C), carrier gas: hydrogen (linear velocity: 30 cm $s^{-1}$), column: DB-5 polyphenylmethylsiloxane (Agilent technologies, Santa Clara, USA) (30 m, 0.25 mm, 0.25 μm), detector temperature 320 °C.

For oleic acid, the oven temperature was set to 180 °C for 2 min, then raised to 240 °C at a speed of 15 K $min^{-1}$, held for 6 min and finally increased to 300 °C at a rate of 20 K $min^{-1}$ and kept at this temperature for 2 min. For linoleic acid, palmitoleic acid, myristoleic acid, (*Z*)-undec-9-enoic acid and dec-9-enoic acid, the oven temperature was set to 50 °C for 2 min, then raised to 100 °C at a speed of 10 K $min^{-1}$, subsequently raised to 200 °C with a rate of 30 K $min^{-1}$ and raised moreover to 240 °C at a speed of 10 K $min^{-1}$. Finally, the temperature was increased to 300 °C at 40 K $min^{-1}$ and held for 3 min.

GC–MS analysis was performed on a Shimadzu GC2010 system (Shimadzu, Kyōto, JP) equipped with a GCMS-QP2010 mass selective detector (electron impact, 70 eV), AOC 5000 autosampler/autoinjector (injection volume: 1 μL, split ratio: 1:20, injection temperature: 250 °C), carrier gas: helium (linear velocity: 30 cm $s^{-1}$), column: ZB-5 polyphenylmethylsiloxane (Zebron – Phenomenex, Torrance, USA) (30 m, 0.25 mm, 0.25 μm), detector temperature: 320 °C); MS: ion source temperature 200 °C, interface temperature 285 °C. The oven temperature was set to 50 °C for 2 min, and then raised to 100 °C at a speed of 10 K $min^{-1}$, subsequently raised to 200 °C with a rate of 30 K $min^{-1}$ and raised moreover to 240 °C at a speed of 10 K $min^{-1}$. Finally, the temperature was increased to 300 °C at 40 K $min^{-1}$ and held for 10 min.

### 2.7. ThermoFAD

The thermostability of OAHs was measured by ThermoFAD according to a protocol published elsewhere [34,35]. The protein lysate samples (25 μL) were heated in a microwell plate using a real-time PCR machine (Eppendorf Mastercycler epgradient S, Hamburg, DE). The temperature was increased stepwise at 0.5 K from 20 °C to 90 °C. During the unfolding process of the proteins, FAD is released and the fluorescence signal was measured at 543 nm. The melting point was determined from the minimum of the second derivation of the fluorescence signal. ThermoFAD was performed in triplicates of the same lysate.

### 2.8. Freeze-drying and determination of residual activity

Cells were sonicated in 50 mM ammonium acetate buffer (pH 7.5) as described above. The obtained lysate was frozen in liquid nitrogen and lyophilized for five days using a freeze-dryer (Christ Alpha 2–4LD plus, Martin Christ Gefriertrocknungsanlagen, Osterode am Harz, DE). The lyophilized proteins were resolved in 50 mM potassium phosphate buffer (pH 6.5) and the residual activity was determined by comparing product formation in biotransformations (cf. 2.6) regarding the conversion of 500 μM oleic acid (1 h, 37 °C, final protein concentration: 0.5 g $L^{-1}$) using fresh lysate or resuspended lyophilisate.

### 2.9. Synthesis of (Z)-undec-9-enoic acid

In a dry Schlenk tube, 9-undecynoic acid (0.48 g, 2.64 mmol) was added to Lindlar catalyst (0.06 g) dissolved in 15 mL methanol (dried over 3 Å molecular sieve) and stirred at room temperature. The atmosphere was replaced ten times with hydrogen by subsequent evacuation and hydrogen flooding. Afterwards, hydrogen was allowed to pass through the reaction mixture for 20 h. Finally, the grey mixture was filtered over celite, washed with methanol and the filtrate was concentrated *in vacuo* to yield a yellowish oil which was purified by column chromatography (cyclohexane/MTBE 5:1, $R_f$ = 0.36, vanillin) to yield (*Z*)-undec-9-enoic acid (0.18 g, 0.98 mmol, 38 %) as a colorless oil (>95 % $^1$H NMR purity).

$^1$H NMR (500 MHz, $CDCl_3$): δ = 1.32–1.35 (m, 8H, 4-H, 5-H, 6-H, 7-H), 1.60 (d, *J* = 6.3 Hz, 3H, 11-H), 1.62–1.65 (m, 2H, 3-H), 2.00–2.04 (m, 2H, 8-H), 2.35 (t, *J* = 7.5 Hz, 2H, 2-H), 5.36-5.40 (m, 2H, 9-H, 10-H) ppm.$^{13}$C NMR (125 MHz, $CDCl_3$): δ = 12.8, 24.7, 26.8, 29.0, 29.0, 29.1, 29.5, 33.9, 123.7, 130.8, 179.6 ppm. FT-IR (ATR): $\tilde{\nu}$ = 3013 (w), 2924 (m), 2855 (m), 1705 (s), 1412 (m), 1284 (m), 1245 (m), 1114 (w), 934 (m), 700 (m) $cm^{-1}$.

## 3. Results and discussion

### 3.1. Database assembly

The *Hydratase Engineering Database* (https://hyed.biocatnet.de) was established in the framework of our in-house database system BioCatNet [25]. The database includes 2046 sequences and thereby increases the number of previously known putative hydratases noteably. These sequences were assigned to eleven homologous families (HFam1-11) sharing a high sequence similarity (average global sequence identity of 62 % inside the families) (Fig. 1). HFam2 constitutes the largest homologous family (1188 sequences) and includes the *Lactobacillus acidophilus* oleate hydratase (*La*-OAH1, pdb entries 4IA5 and 4IA6). The next larger families are HFam1 (436 sequences) and HFam3 (191 sequences). HFam11 (116 sequences) contains the *Elizabethkingia meningoseptica* oleate hydratase *(Em*-OAH1, pdb entry 4UIR). For all other homologous families (HFam4-10), no structure information is available. These families contain less than 50 sequences each. The putative OAHs were mainly derived from bacterial sources, but also 103 fungal and 24 archaeal sequences are included in the database (Fig. S1).

To identify structurally and functionally important positions, the homologous families were investigated for similarities and for systematic differences in their conservation patterns. 80 Positions were found to be highly conserved among all sequences (identical amino acids in >90 % of the sequences, Fig. S2, Table S9).

Some of these conserved positions have been described in literature before: The glycine-rich motif of the Rossmann-fold (usually described as GxGxxG) was described as GxGxx[**G**SAN]x(15)[**E**KD]x(5)[**E**DGS] for OAHs based on a sequence alignment using ten enzymes [4]. The conservation analysis

Please cite this article in press as: J. Schmid, et al., Biocatalytic study of novel oleate hydratases, J. Mol. Catal. B: Enzym. (2017), http://dx.doi.org/10.1016/j.molcatb.2017.01.010

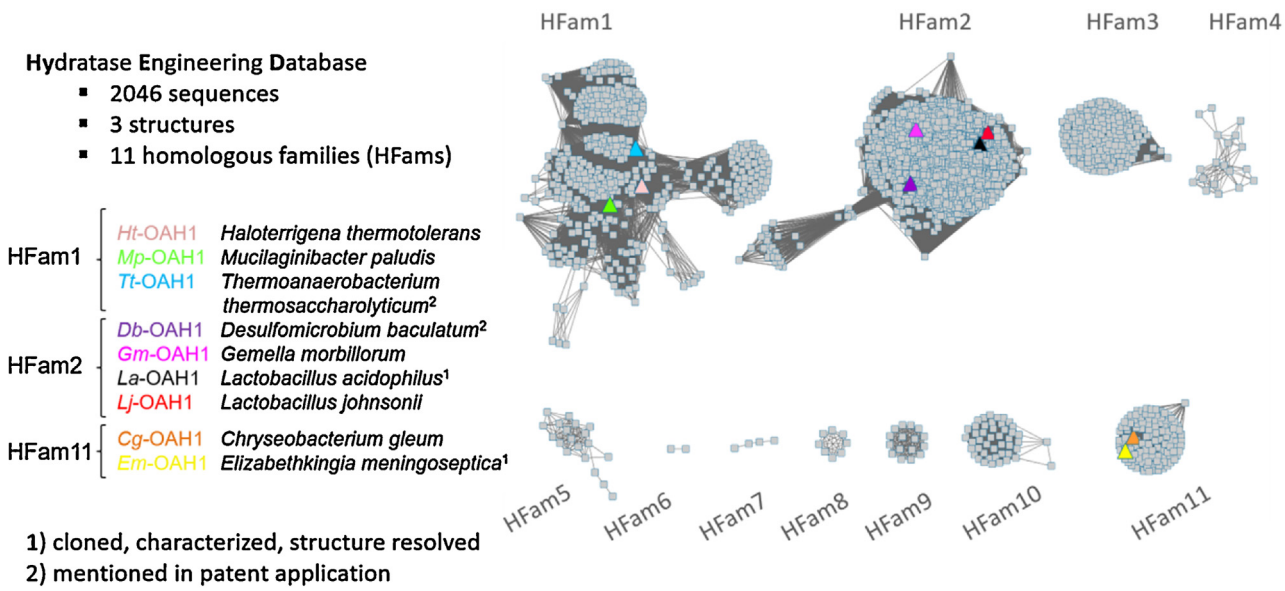


**Fig. 1.** Sequence similarity network of the HyED showing the classification into eleven homologous families (HFams). The previously characterized oleate hydratase from *Lactobacillus acidophilus* (black) is found in HFam2, while the oleate hydratase from *Elizabethkingia meningoseptica* (yellow) is found in HFam11. The sequences selected for characterization are from HFam1, HFam2 and HFam11 and shown as colored triangles.

based on all sequences of the HyED shows that this region is even more conserved than indicated by the sequence pattern derived from literature: for 16 of the 28 positions described by this motif, already two amino acids are sufficient to describe 90 % of the OAHs (Table S10). A more specific and sensitive sequence motif for the FAD-cofactor binding region of OAHs is $G_{69}$xG[LI][**A**G]x[**L**M][**A**S][**A**G]Ax[**F**Y][**L**M][**I**V]**R**[**D**E][**G**A]x(3)**G**x[**I**V]x[**I**FVL][**L**FY]$\mathbf{E}_{96}$ (positions according to *Em*-OAH1). Interestingly, the motif derived from literature describes a charged residue at position 90 (position underlined in both sequence motifs). Due to our criteria no residue is conserved at this position, but a tendency can be seen (35 % E, 16 % K, 15 % S, 14 % D, 5 % Q, 4 % N). For some of the positions found in the cofactor binding region, specific functions were reported in previous studies [36,37]. The conserved glycines at positions 69 and 71 were described to facilitate the positioning of the FAD. Further, residues at positions 78 and 74 were reported to stabilize the interaction between the first β-strand and the following α-helix [36,37]. However, although a tendency towards small amino acids can be seen for position 74, no residue is found to be conserved.

Of the other regions conserved in OAHs, the loop region $R_{118}$GGREM$_{123}$ (positions according to *Em*-OAH1) has been described to have a structural role for cofactor binding and an additional role in catalysis has been proposed for E122 [19]. Indeed, this region is highly conserved among all database members (Table S11). Other highly conserved residues in *Em*-OAH1 are Y241, which was also proposed to be involved in the reaction [19] and the residues suggested to bind the carboxylate of the oleate substrate (Q265, T436, N438 and H442) [19].

Interestingly, some of these positions showed a family specific conservation (Table S12). Instead of the proposed catalytic glutamic acid at position 122, methionine is conserved in HFam1. HFam1 also forms an exception at position 123 where predominantly leucine is found, as well as at the position 436 where valine is conserved and position 438 where predominantly small residues are found.

For none of the other conserved or family-specific conserved positions, a function has been proposed yet. However, several of them can be found in the substrate binding pocket and thus, are supposed to contribute to substrate binding or catalysis.

### 3.2. Selection of homologs

Representative OAHs were selected from literature and our database (Fig. 1) for the comparative investigation of properties interesting for biocatalysis including stability, activity and substrate specificity. The two already described oleate hydratases *La*-OAH1 [18] (HFam2) and *Em*-OAH1 [19] (HFam11) for which also structural information is available, as well as representative homologs from these families were chosen: The putative oleate hydratases from *Lactobacillus johnsonii* (*Lj*-OAH1), *Gemella morbillorum* (*Gm*-OAH1) and *Desulfomicrobium baculatum* (*Db*-OAH1) [24] from HFam2 were selected for their high sequence similarity to *La*-OAH1. *Chryseobacterium gleum* (*Cg*-OAH1) from HFam11 was chosen for its high sequence similarity to *Em*-OAH1. Since members of HFam1 show an interesting family-specific conservation, three additional putative oleate hydratases from the thermophilic archaeon *Haloterrigena thermotolerans* (*Ht*-OAH1), from the thermophilic bacterium *Mucilaginibacter paludis* (*Mp*-OAH1) and from *Thermoanaerobacterium thermosaccharolyticum* (*Tt*-OAH1) [24] were selected, especially for their potentially increased (thermo)stability.

### 3.3. Activity, regioselectivity and stability

The nine selected genes were cloned into pET28a(+) vector for expression in *E. coli* BL21 (DE3). A small expression study was performed to optimize several parameters including incubation temperature, time and induction method. The improved expression procedure was then utilized to investigate the overexpression capability and the individual expression levels were compared (Figure S3). Overexpression was detectable for seven out of nine homologous genes (~65 kDa). Two hydratase genes from *Haloterrigena thermotolerans* and *Thermoanaerobacterium thermosaccharolyticum* showed no expression. The expression of the oleate hydratase genes from *Mucilaginibacter paludis* and *Lactobacillus johnsonii* led to the formation of inclusion bodies. The five oleate hydratases from *Chryseobacterium gleum*, *Desulfomicrobium baculatum*, *Elizabethkingia meningoseptica*, *Gemella morbillorum* and *Lactobacillus acidophilus* showed good overexpression.

Please cite this article in press as: J. Schmid, et al., Biocatalytic study of novel oleate hydratases, J. Mol. Catal. B: Enzym. (2017), http://dx.doi.org/10.1016/j.molcatb.2017.01.010

Activity tests were performed with oleic acid (C18:1) as substrate. Four hydratases showed moderate to high conversion (*Cg*-OAH1: 87 %, *Db*-OAH1: 26 %, *Em*-OAH1 89 % and *La*-OAH1: 33 %), one hydratase (*Gm*-OAH1) showed only minor conversion (2 %). *Lj*- and *Mp*-OAH1 formed inclusion bodies during expression. No activity was detected for lysates of cells showing no overexpression in SDS-PAGE. Negative controls were performed using lysate of induced cells containing empty pET28a(+) vector.

In order to characterize the enzyme panel regarding regioselectivity, the active homologs were incubated with linoleic acid (C18:2) and the fragmentation patterns of the hydrated products were analyzed via GC–MS. The five enzymes were also active with linoleic acid, forming the 10-hydroxy product (Table 1).

To analyze robustness, we investigated thermostability and residual activity after freeze-drying (Table S13). All homologs showed comparable melting points $T_m$ ranging from 56.0 ± 0.2 °C for *La*-OAH1 to 65.6 ± 0.2 °C for *Em*-OAH1. This is in accordance with a study of the *Lysinibacillus fusiformis* oleate hydratase demonstrating that the enzyme was stable at 40 °C for 1 h showing increasingly faster denaturation for temperatures between 40 and 70 °C [38]. Clear differences in their behavior were measurable by comparing their activity for the hydration of oleic acid under the same conditions before and after freeze-drying. *Db*- and *Gm*-OAH1 lost a majority of their initial activity. After freeze-drying only 17 % or 15 %, respectively, were detectable. *La*-OAH1 retained 57 %, whereas *Cg*- and *Em*-OAH1 out of HFam11 where clearly not as much affected as the other enzymes from HFam2. *Cg*-OAH1 lost 9 % activity and *Em*-OAH1 only 7 %.

### 3.4. Optimization of reaction conditions

The reported pH-optima for most of the oleate hydratases is in the range from pH 5.5–6.8[38–40]. Therefore we used potassium phosphate buffer pH 6.5 for our initial tests. However, in addition to the pH, enzyme stability becomes increasingly important for the biotransformation of non-natural substrates with prolonged reaction time and higher protein concentration. It was not possible under standard conditions with potassium phosphate buffer to monitor any oleate hydratase reaction longer than two days. Blurring of the reaction mixture after 1 d indicated the beginning denaturation of the enzymes from the cell lysate leading to the exposure of hydrophobic areas and the subsequent interaction with substrate and product. As a result, neither substrate nor product were detectable in the extract of the reaction mixture. Hence, we compared the product formation for the biotransformation of myristoleic acid (C14:1) over 1 d and 2 d in four different buffer systems at pH 6.0 (potassium phosphate, citrate, BIS-TRIS, MES) using *Em*-OAH1. The experiments showed that the product recovery in the 2 d sample was less than in the 1 d sample for potassium phosphate and BIS-TRIS, while more product was isolated after 2 d for citrate and MES buffer. Particularly, the obtained product decreased for potassium phosphate from 100 % to 58 % and for BIS-TRIS from 105 % to 78 %, whereas increased from 122 % to 134 % and 114 % to 148 % for citrate and MES buffer, respectively. The percentages are all normalized to the product formation after 1 d in 50 mM potassium phosphate buffer pH 6.0.

From the tested buffer systems, we chose 50 mM citrate buffer pH 6.0 for higher stability of oleate hydratases at prolonged reaction times and better reproducibility of long-term experiments.

### 3.5. Substrate scope analysis

The so far investigated substrate scope described in literature and the applied reaction conditions often differ for each individual homolog, which makes it difficult to compare the different enzymes. Furthermore, different enzyme preparations ranging from whole cells over cell-free extract to purified enzymes are utilized [19,39,41,42]. In the case of fatty acids, this can have a huge impact on the performance of biotransformations as the long-chain substrates have to be actively imported in the case of whole cells, whereas cell-free protein extract does not face this limitation [43,44]. Therefore we preferred cell-free protein extract over whole cells for studying the substrate scope. In order to obtain comparable results we focused on the substrate panel shown in Table 1. This set comprises six different substrates. Starting from the C18 substrates oleic acid and linoleic acid, the latter used for the determination of the regioselectivity, we continued with successively shorter substrates. Biotransformations were performed for these substrates with all cloned enzymes regardless of their expression behavior. Consistent with the SDS-PAGE (Fig. S3), which showed no overexpression for the hydratases from the thermophilic organisms, no activity could be detected for the enzymes from *Haloterrigena thermotolerans* (*Ht*-OAH1) and *Thermoanaerobacterium thermosaccharolyticum* (*Tt*-OAH1) towards any of the substrates. This was also the case for *Mp*-OAH1 from *Mucilaginibacter paludis* and *Lj*-OAH1 from *Lactobacillus johnsonii* because of the formation of inclusion bodies. Negative controls were performed using lysate of induced cells containing an empty pET28a(+) vector.

The activity of OAHs for the natural substrate oleic acid (C18:1) was high, leading to a conversion of up to 90 % after 5 min. Nevertheless, due to the different kinetics for each substrate, the reaction conditions had to be adjusted accordingly in terms of reaction time and enzyme concentration. The different parameters and results of the biotransformations are listed in Table 1.

Oleic acid (C18:1) was the best substrate and high conversions were reached with *Cg*-OAH1 and *Em*-OAH1, moderate product formation was observed with *Db*-OAH1 and *La*-OAH1 whereas *Gm*-OAH1 was almost inactive at protein concentrations of 0.15 g $L^{-1}$ and reaction times of 5 min. With shorter chain lengths of the substrates, the reaction times were prolonged and the enzyme concentrations were increased to reach a substantial and comparable amount of product. For the short-chain substrates (*Z*)-undec-9-enoic acid (C11:1) and dec-9-enoic acid (C10:1) the protein concentration was increased to 4 g $L^{-1}$ and the reaction time prolonged to 5 d.

Interestingly, *Gm*-OAH1 (*Gemella morbillorum*) was more active on the shorter chain substrates relative to the homologous enzymes compared with the biotransformation of oleic acid (Table 1).

The remaining active homologs behaved relatively similar when compared amongst each other. However, some remarkable differences are recognizable. The two hydratases from *Lactobacillus acidophilus* (*La*-OAH1) and *Desulfomicrobium baculatum* (*Db*-OAH1) exhibited a lower activity towards the long-chain substrates C18:1 and C18:2 but showed comparable high activity to the medium chain substrates C16:1 and C14:1. *Gm*-OAH1, also found in HFam2, displayed even lower activity on linoleic acid (C18:2) and oleic acid (C18:1), but had a relative high or increased activity towards substrates of shorter chain length. The two homologous enzymes from *Chryseobacterium gleum* and *Elizabethkingia meningoseptica* demonstrated a good overall performance throughout the substrate panel ranging from C18:2 to C14:1 and displayed together with *Gm*-OAH1 the highest conversion for the short-chain substrate (*Z*)-undec-9-enoic acid (C11:1). Whereas *Gm*-OAH1 was able to form 16 % of the corresponding 10-hydroxyundecanoic acid, *Em*-OAH1 and *Cg*-OAH1 were able to produce almost the double amount (23 % and 30 %).

Despite their activity on *9Z*-double bonds, the homologous enzymes were also characterized on their capability to hydrate a terminal double bond as in dec-9-enoic acid (C10:1). However, none of the homologs was active towards this substrate.

*Cg*-OAH1 and *Em*-OAH1, both found in HFam11, could be identified as enzymes with the highest activity on all substrates. The

Please cite this article in press as: J. Schmid, et al., Biocatalytic study of novel oleate hydratases, J. Mol. Catal. B: Enzym. (2017), http://dx.doi.org/10.1016/j.molcatb.2017.01.010

**Table 1**
Substrate scope analysis of putative oleate hydratases. Product formation [%], reaction time and protein concentration of biotransformations.

| structure | substrate | abbrev. | *Db* | *Gm* | *La* | *Cg* | *Em* |
|---|---|---|---|---|---|---|---|
| 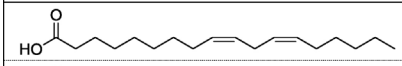 | linoleic acid | C18:2[(a)] | 49 ± 5 | 18 ± 5 | 38 ± 3 | 87 ± 8 | 85 ± 22 |
| 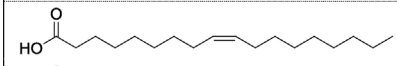 | oleic acid | C18:1[(b)] | 26 ± 4 | 2 ± 0.2 | 33 ± 3 | 87 ± 4 | 89 ± 8 |
| 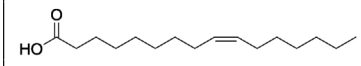 | palmitoleic acid | C16:1[(c)] | 95 ± 6 | 37 ± 1 | 91 ± 5 | 93 ± 12 | 95 ± 4 |
| 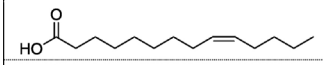 | myristoleic acid | C14:1[(d)] | 77 ± 8 | 80 ± 3 | 90 ± 3 | 95 ± 6 | 93 ± 3 |
| 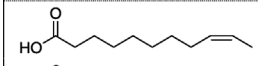 | (*Z*)-undec-9-enoic acid | C11:1[(e)] | 2 ± 0.03 | 16 ± 1 | 4 ± 0.2 | 30 ± 1 | 23 ± 2 |
| 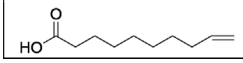 | dec-9-enoic acid | C10:1[(f)] | - | - | - | - | - |

Product formation is indicated as follows: no highlighting (< 20 %), light grey (20–34 %), grey (35–74 %), dark grey (> 75 %). Reaction times ($t_{reaction}$) and protein concentrations ($c_{protein}$): [(a)] 4.5 h, 0.5 g L$^{-1}$, [(b)] 5 min, 0.15 g L$^{-1}$, [(c)] 30 min, 0.5 g L$^{-1}$, [(d)] 21 h, 2 g L$^{-1}$, [(e/f)] 5 d, 4 g L$^{-1}$.

enzymes of HFam2 on the other hand showed only high yields for fatty acids of medium chain length (C14 and C16) under the tested conditions. Therefore, enzymes of HFam11 are particularly interesting for further investigations and for the applications as hydration catalyst for short-chain fatty acids and alkenes.

## 4. Conclusion

In this study, we established the publicly available *Hydratase Engineering Database* (HyED) to serve as navigation tool and to collect information about this interesting protein family. Particularly, we examined the oleate hydratase family around the enzymes from *Elizabethkingia meningoseptica* and *Lactobacillus acidophilus* in further detail and used the HyED for the investigation of conserved sequence motifs to gain further insights into the molecular base of these enzymes.

Furthermore, we have chosen nine homologous oleate hydratases for detailed investigations and heterologously expressed them in *E. coli*. Five homologous genes were suitable for clear and stable overexpression. The enzymes were analyzed with a set of substrates, ranging from long-chain to medium-chain fatty acids. For the first time, we have tested two novel substrates (C11:1 and C10:1) and activity could be demonstrated towards (*Z*)-undec-9-enoic acid (C11:1). All actively expressed hydratases can be classified for their comparable substrate scope as oleate hydratases.

The oleate hydratases from HFam11, *Em*-OAH1 and *Cg*-OAH1, showed the highest stability as well as activity towards the novel non-natural shorter chained substrates. This makes them ideal candidates for further mutagenesis experiments with the goal to evolve a hydration biocatalyst with improved properties. We believe that using the inherent hydration potential of oleate hydratases can lead to new chemistry and, beyond, can provide an alternative to chemical synthesis, not only for hydroxy fatty acids but also for the formation of chiral alcohols starting from alkenes/double bonds.

## Acknowledgements

The research leading to these results has received funding from the Ministry for Science, Research and the Arts of Baden-Württemberg, Germany [MWK; Baden-Württemberg Biosynthesis netWork (BW$^2$)]. Furthermore we want to thank Constantin Vogel for the initial work on the hydratase engineering database and Linda Otten (TU Delft) for helpful discussions. Moreover we would like to give our special thanks to Bettina Nestl for her tremendous support and discussions throughout the writing process of this publication.

## Appendix A. Supplementary data

Supplementary data associated with this article can be found, in the online version, at http://dx.doi.org/10.1016/j.molcatb.2017.01.010.

## References

[1] V. Resch, U. Hanefeld, The selective addition of water, Catal. Sci. Technol. 5 (2015) 1385–1399, http://dx.doi.org/10.1039/C4CY00692E.
[2] B.N.M. van Leeuwen, A.M. van der Wulp, I. Duijnstee, A.J.A. van Maris, A.J.J. Straathof, Fermentative production of isobutene, Appl. Microbiol. Biotechnol. 93 (2012) 1377–1387, http://dx.doi.org/10.1007/s00253-011-3853-7.
[3] J. Jin, U. Hanefeld, The selective addition of water to CC bonds; enzymes are the best chemists, Chem. Commun. (Camb.) 47 (2011) 2502–2510, http://dx.doi.org/10.1039/c0cc04153j.
[4] A. Hiseni, I.W.C.E. Arends, L.G. Otten, New cofactor-independent hydration biocatalysts: structural, biochemical, and biocatalytic characteristics of carotenoid and oleate hydratases, ChemCatChem 7 (2015) 29–37, http://dx.doi.org/10.1002/cctc.201402511.
[5] Z. Sun, S. Shen, C. Wang, H. Wang, Y. Hu, J. Jiao, T. Ma, B. Tian, Y. Hua, A novel carotenoid 1 2-hydratase (CruF) from two species of the non-photosynthetic bacterium Deinococcus, Microbiology 155 (2009) 2775–2783, http://dx.doi.org/10.1099/mic.0.027623-0.
[6] S. Steiger, A. Mazet, G. Sandmann, Heterologous expression, purification, and enzymatic characterization of the acyclic carotenoid 1,2-hydratase from Rubrivivax gelatinosus, Arch. Biochem. Biophys. 414 (2003) 51–58, http://dx.doi.org/10.1016/S0003-9861(03)00099-7.
[7] D. Brodkorb, M. Gottschall, R. Marmulla, F. Lüddeke, J. Harder, Linalool dehydratase-isomerase, a bifunctional enzyme in the anaerobic degradation of monoterpenes, J. Biol. Chem. 285 (2010) 30436–30442, http://dx.doi.org/10.1074/jbc.M109.084244.
[8] L.E. Bevers, M.W.H. Pinkse, P.D.E.M. Verhaert, W.R. Hagen, Oleate hydratase catalyzes the hydration of a nonactivated carbon–carbon bond, J. Bacteriol. 191 (2009) 5010–5012, http://dx.doi.org/10.1128/J.B.00306-09.
[9] L.L. Wallen, R.G. Benedict, R.W. Jackson, The microbiological production of 10-Hydroxystearic acid from oleic acid, Arch. Biochem. Biophys. 99 (1962) 249–253, http://dx.doi.org/10.1016/0003-9861(62)90006-1.
[10] S. Koritala, C.T. Hou, C.W. Hesseltine, M.O. Bagby, Microbial conversion of oleic acid to 10-hydroxystearic acid, Appl. Microbiol. Biotechnol. 32 (1989) 299–304, http://dx.doi.org/10.1007/BF00184978.
[11] G.J. Schroepfer, K. Bloch, The stereospecific conversion of stearic acid to oleic acid, J. Biol. Chem. 240 (1965) 54–63.
[12] W.G. Niehaus, A. Torkelson, A. Kisic, D.J. Bednarczyk, G.J. Schroepfer, Stereospecific hydration of the delta-9 double bond of oleic acid, J. Biol. Chem. 245 (1970) 3790–3797.
[13] W.G. Niehaus, G.J. Schroepfer, The reversible hydration of oleic acid to 10D-hydroxystearic acid, Biochem. Biophys. Res. Commun. 21 (1965) 271–275, http://dx.doi.org/10.1016/0006-291X(65)90282-2.
[14] Y.-C. Joo, K.-W. Jeong, S.-J. Yeom, Y.-S. Kim, Y. Kim, D.-K. Oh, Biochemical characterization and FAD-binding analysis of oleate hydratase from Macrococcus caseolyticus, Biochimie 94 (2012) 907–915, http://dx.doi.org/10.1016/j.biochi.2011.12.011.
[15] J.-Y. Park, S.-H. Lee, K.-R. Kim, J.-B. Park, D.-K. Oh, Production of 13S-hydroxy-9(*Z*)-octadecenoic acid from linoleic acid by whole recombinant

cells expressing linoleate 13-hydratase from Lactobacillus acidophilus, J. Biotechnol. 208 (2015) 1–10, http://dx.doi.org/10.1016/j.jbiotec.2015.05.006.
[16] A. Kisic, Y. Miura, G.J. Schroepfer, Oleate hydratase: studies of substrate specificity, Lipids 6 (1971) 541–545, http://dx.doi.org/10.1007/BF02531133.
[17] T. Kaneshiro, J.-K. Huang, D. Weisleder, M. Bagby, 10(R)-Hydroxystearic acid production by a novel microbe, NRRL B-14797, isolated from compost, J. Ind. Microbiol. 13 (1994) 351–355, http://dx.doi.org/10.1007/BF01577218.
[18] A. Volkov, S. Khoshnevis, P. Neumann, C. Herrfurth, D. Wohlwend, R. Ficner, I. Feussner, Crystal structure analysis of a fatty acid double-bond hydratase from Lactobacillus acidophilus, Acta Crystallogr. D. Biol. Crystallogr. 69 (2013) 648–657, http://dx.doi.org/10.1107/S0907444913000991.
[19] M. Engleder, T. Pavkov-Keller, A. Emmerstorfer, A. Hromic, S. Schrempf, G. Steinkellner, T. Wriessnegger, E. Leitner, G.A. Strohmeier, I. Kaluzna, D. Mink, M. Schürmann, S. Wallner, P. Macheroux, K. Gruber, H. Pichler, Structure-based mechanism of oleate hydratase from Elizabethkingia meningoseptica, Chembiochem 16 (2015) 1730–1734, http://dx.doi.org/10.1002/cbic.201500269.
[20] F.C. Naughton, Production, chemistry, and commercial applications of various chemicals from castor oil, J. Am. Oil Chem. Soc. 51 (1974) 65–71, http://dx.doi.org/10.1007/BF00000015.
[21] Y. Wache, M. Aguedo, A. Choquet, I.L. Gatfield, J.-M. Nicaud, J.-M. Belin, Role of beta-Oxidation Enzymes in gamma-Decalactone Production by the Yeast Yarrowia lipolytica, Appl. Environ. Microbiol. 67 (2001) 5700–5704, http://dx.doi.org/10.1128/AEM.67.12.5700-5704.2001.
[22] J.W. Song, E.Y. Jeon, D.H. Song, H.Y. Jang, U.T. Bornscheuer, D.K. Oh, J.B. Park, Multistep enzymatic synthesis of long-chain α, ω-dicarboxylic and ω-hydroxycarboxylic acids from renewable fatty acids and plant oils, Angew. Chem. Int. Ed. 52 (2013) 2534–2537, http://dx.doi.org/10.1002/anie.201209187.
[23] J.W. Song, J.H. Lee, U.T. Bornscheuer, J.B. Park, Microbial synthesis of medium-chain α, ω-dicarboxylic acids and ω-aminocarboxylic acids from renewable long-chain fatty acids, Adv. Synth. Catal. 356 (2014) 1782–1788, http://dx.doi.org/10.1002/adsc.201300784.
[24] P. Marliere, Method for Producing an Alkene Comprising the Step of Converting an Alcohol by an Enzymatic Dehydration Step, WO2011/076691A1/EP2336341A1, (2011).
[25] P. Buchholz, C. Vogel, W. Reusch, M. Pohl, D. Rother, A. Spieß, J. Pleiss, BioCatNet: a database system for the integration of enzyme sequences and biocatalytic experiments, Chembiochem (2016), http://dx.doi.org/10.1002/cbic.201600462.
[26] S.F. Altschul, T.L. Madden, A.A. Schäffer, J. Zhang, Z. Zhang, W. Miller, D.J. Lipman, Gapped BLAST and PSI-BLAST: a new generation of protein database search programs, Nucleic Acids Res. 25 (1997) 3389–3402, http://dx.doi.org/10.1093/nar/25.17.3389.
[27] D.A. Benson, M. Cavanaugh, K. Clark, I. Karsch-Mizrachi, D.J. Lipman, J. Ostell, E.W. Sayers, GenBank. Nucleic Acids Res. 41 (2013) D36–D42, http://dx.doi.org/10.1093/nar/gks1195.
[28] R.C. Edgar, Search and clustering orders of magnitude faster than BLAST, Bioinformatics 26 (2010) 2460–2461, http://dx.doi.org/10.1093/bioinformatics/btq461.
[29] S.B. Needleman, C.D. Wunsch, A general method applicable to the search for similarities in the amino acid sequence of two proteins, J. Mol. Biol. 48 (1970) 443–453, http://dx.doi.org/10.1016/0022-2836(70)90057-4.
[30] P. Shannon, A. Markiel, O. Ozier, N.S. Baliga, J.T. Wang, D. Ramage, N. Amin, B. Schwikowski, T. Ideker, Cytoscape: a software environment for integrated models of biomolecular interaction networks, Genome Res. 13 (2003) 2498–2504, http://dx.doi.org/10.1101/gr.1239303.
[31] H.M. Berman, The protein data bank, Nucleic Acids Res. 28 (2000) 235–242, http://dx.doi.org/10.1093/nar/28.1.235.
[32] F. Sievers, A. Wilm, D. Dineen, T.J. Gibson, K. Karplus, W. Li, R. Lopez, H. McWilliam, M. Remmert, J. Soding, J.D. Thompson, D.G. Higgins, Fast, scalable generation of high-quality protein multiple sequence alignments using Clustal Omega, Mol Syst. Biol. 7 (2014) 539, http://dx.doi.org/10.1038/msb.2011.75.
[33] U.K. Laemmli, Cleavage of structural proteins during the assembly of the head of bacteriophage T4, Nature 227 (1970) 680–685, http://dx.doi.org/10.1038/227680a0.
[34] F. Forneris, R. Orru, D. Bonivento, L.R. Chiarelli, A. Mattevi, Thermo FAD, a Thermofluor® −adapted flavin ad hoc detection system for protein folding and ligand binding, FEBS J. 276 (2009) 2833–2840, http://dx.doi.org/10.1111/j.1742-4658.2009.07006.x.
[35] S. Reich, N. Kress, B.M. Nestl, B. Hauer, Variations in the stability of NCR ene reductase by rational enzyme loop modulation, J. Struct. Biol. 185 (2014) 228–233, http://dx.doi.org/10.1016/j.jsb.2013.04.004.
[36] G. Kleiger, D. Eisenberg, GXXXG and GXXXA Motifs Stabilize FAD and NAD(P)-binding Rossmann Folds Through Cα-H-O Hydrogen Bonds and van der Waals Interactions, J. Mol. Biol. 323 (2002) 69–76, http://dx.doi.org/10.1016/S0022-2836(02)00885-9.
[37] R.K. Wierenga, P. Terpstra, W.G. Hol, Prediction of the occurrence of the ADP-binding beta alpha beta-fold in proteins, using an amino acid sequence fingerprint, J. Mol. Biol. 187 (1986) 101–107, http://dx.doi.org/10.1016/0022-2836(86)90409-2.
[38] M.-H. Seo, K.-R. Kim, D.-K. Oh, Production of a novel compound 10,12-dihydroxystearic acid from ricinoleic acid by an oleate hydratase from Lysinibacillus fusiformis, Appl. Microbiol. Biotechnol. 97 (2013) 8987–8995, http://dx.doi.org/10.1007/s00253-013-4728-x.
[39] M. Takeuchi, S. Kishino, A. Hirata, S.-B. Park, N. Kitamura, J. Ogawa, Characterization of the linoleic acid Δ9 hydratase catalyzing the first step of polyunsaturated fatty acid saturation metabolism in Lactobacillus plantarum AKU, J. Biosci. Bioeng. 119 (2015) (2015) 636–641, http://dx.doi.org/10.1016/j.jbiosc.2014.10.022.
[40] C.T. Hou, Production of hydroxy fatty acids from unsaturated fatty acids by flavobacterium sp. DS5 hydratase, a C-10 positional- and cis unsaturation-specific enzyme, J. Am. Oil Chem. Soc. 72 (1995) 1265–1270, http://dx.doi.org/10.1007/BF02546197.
[41] M.H. Kim, M.S. Park, C.H. Chung, C.T. Kim, Y.S. Kim, K.H. Kyung, Conversion of unsaturated food fatty acids into hydroxy fatty acids by lactic acid bacteria, J. Microbiol. Biotechnol. 13 (2003) 360–365.
[42] I.-S. Yu, H.-J. Kim, D.-K. Oh, Conversion of linoleic acid into 10-Hydroxy-12(*Z*)-octadecenoic acid by whole cells of stenotrophomonas nitritireducens, Biotechnol. Prog. 24 (2008) 182–186, http://dx.doi.org/10.1021/bp0703073.
[43] W.D. Nunn, R.W. Simons, Transport of long-chain fatty acids by Escherichia coli: mapping and characterization of mutants in the fadL gene, Proc. Natl. Acad. Sci. 75 (1978) 3377–3381.
[44] J.H. Bae, B.G. Park, E. Jung, P.-G. Lee, B.-G. Kim, fadD deletion and fadL overexpression in Escherichia coli increase hydroxy long-chain fatty acid productivity, Appl. Microbiol. Biotechnol. 98 (2014) 8917–8925, http://dx.doi.org/10.1007/s00253-014-5974-2.

Please cite this article in press as: J. Schmid, et al., Biocatalytic study of novel oleate hydratases, J. Mol. Catal. B: Enzym. (2017), http://dx.doi.org/10.1016/j.molcatb.2017.01.010